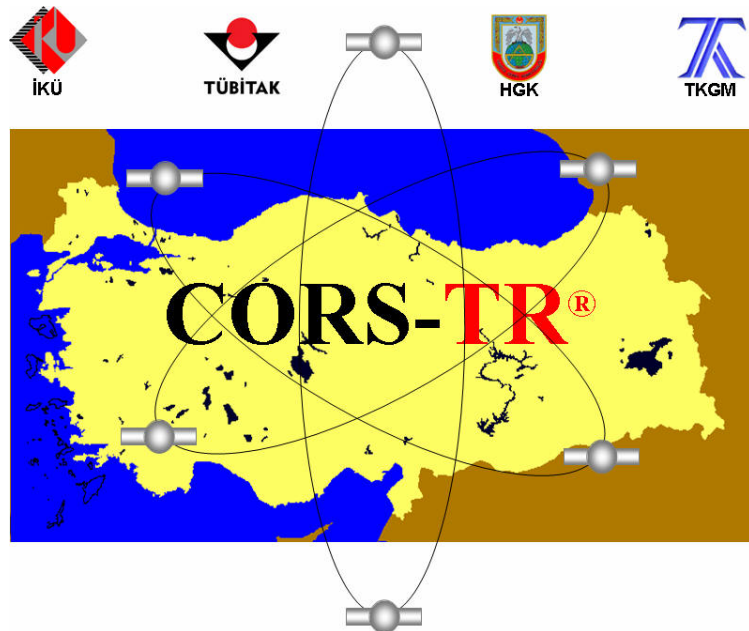


T.C.
İSTANBUL KÜLTÜR UNIVERSITY



ATMOSPHERE PHYSICS LECTURE NOTES

(15th August – 5th September 2006)

Assoc. Prof. Dr. Aysegül YILMAZ
Project Supportive
Researcher
Çanakkale Onsekiz Mart University

Publication No : 1

Contents

CHAPTER 1 : EARTH'S ATMOSPHERIC STRUCTURE

1.1 ATMOSPHERIC LAYERS	1
1.1.1 Troposphere	1
1.1.2 Stratosphere	2
1.1.3 Mesosphere	3
1.1.4 Thermosphere	4
1.1.5 Exosphere	5
1.2 IONOSPHERE	5
1.2.1 Ionospheric Layers	5
1.2.2 Ionospheric Density Profile	7
1.2.3 Aurora	7

CHAPTER 2 : TERRESTRIAL IONOSPHERE AT HIGH LATITUDES

2.1 ELECTROMAGNETIC COUPLING	8
2.2 CONVECTION ELECTRIC FIELDS	9
2.2.1 Convection Models	10
2.3.1 Effects of Convection Model	11
2.3 PARTICLE PRECIPITATION	11
2.4 CURRENT SYSTEMS	12
2.5 LARGE SCALE ATMOSPHERIC STRUCTURES	13
2.6 GEOMAGNETIC STORMS	14
2.7 SUBSTORMS	14
2.8 POLAR WIND	14

CHAPTER 3 : PHYSICS OF NEUTRAL ATMOSPHERE

3.1 PHYSICS LAWS FOR THE NEUTRAL ATMOSPHERE	15
3.1.1 Equation of state	16
3.1.2 Hydrostatic Equilibrium	17
3.1.3 Snell's law	18

3.2 WATER VAPOR	19
3.2.1 Mixing ratio	19
3.2.2 Virtual temperature	20
3.2.3 Partial pressure of saturated air	21
3.2.4 Relative humidity	22
3.3 PROPOGATION DELAY AND REFRACTIVITY	24
3.4 ATMOSPHERIC PROFILES	28
3.4.1 Refractivity profile of dry air	30
3.4.2 Saturation profile	30
CHAPTER 4: PHYSICS OF IONOSPHERE	
4.1 HISTORY	32
4.2 THE REQUIREMENTS FOR AN IONOSPHERE	33
4.3 THE NEUTRAL ATMOSPHERE	34
4.4 ION PRODUCTION	35
4.5 PARTICLE IMPACT IONIZATION	39
4.6 ION LOSS	41
4.7 DETERMINING IONOSPHERIC DENSITY FROM PRODUCTION AND LOSS RATES	41
CHAPTER 5: ATMOSPHERIC WAVE PROPAGATION	
5.1 RADIO WAVE PROPAGATION CHARACTERISTICS	43
5..1.1 REFRACTION	43
5.1.1.1 Layer density	43
5.1.1.2 Frequency	44
5.1.1.3 Angle of incidence and Critical angle	45
5.1.2 REFLECTION	47
5.1.3.DIFRACTION	48
5.2 ATMOSPHERIC EFFECTS ON PROPAGATION	50
5.2.1 REGULAR VARIATIONS	48
5.2.1.1 FADING	48
5.2..1.2 MULTIPATH	49
5.2.1.3 SEASONAL VARIATIONS IN THE IONOSPHERE	50

5.2.1.4 SUNSPOTS	50
5.2.1.4. 1 Twenty-seven day cycle	51
5.2.1.4.2 Eleven-year-cycle	52
5.2.2 IRREGULAR VARIATIONS	52
5.2.2 1 Spodic E	52
5.2.2.2 Sudden Ionospheric Disturbances	53
5.2.2.3 Ionospheric Storms	53
5.3 WEATHER	53
5.3.1.Rain	53
5.3.2 Fog	53
5.3.3 Snow	53
5.3.4 Hail	53
REFERENCES	54

Acknowledgements

We would like to thank Prof.Dr.Turgut UZEL for his invitation to give a seminar on Physics of Ionosphere, Aug.15 and 30, 2006,İstanbul Kültür University, under TÜBİTAK CORS TR Project.

CHAPTER 1 : EARTH'S ATMOSPHERIC STRUCTURE

1. 1 ATMOSPHERIC LAYERS

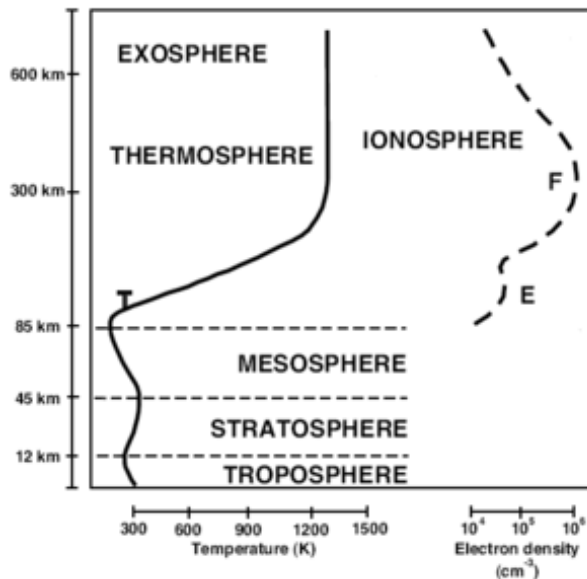


Figure 1.1 Atmospheric Layers

The Earth's atmosphere occupies relatively thin, spherical envelope that extends from the Earth's surface to 1000 km. It is thickest near the Earth's surface and thins out with height until eventually merges with space. Earth's atmosphere varies in density and composition as the altitude increases above the Earth's surface. However, the temperature in the lower atmosphere displays important variations with altitude that act to produce stratified layers, as shown in Fig.1.1.

1.1.1 Troposphere

This first layer above the Earth's surface contains 90% of the Earth's atmosphere and 99% of the water vapor. The gases in this region are predominantly molecular Oxygen(O_2) and molecular nitrogen(N_2). Temperature in this region rapidly and almost linearly decreases with altitude, up to a minimum value, which defines its upper boundary, tropopause. At tropopause, the top of the troposphere at about 9-16 km above mean sea level(msl), the temperature stays constant for about altitude of 10 km. The highest mountains are still within the troposphere and all of our normal day-to-day activities occur here. All atmospheric weather is confined in this lower region



Figure 1.2 Image of the clouds in the Earth's troposphere

Atmospheric weather is a state of the atmosphere at any given time and place. Weather occurs because our atmosphere is in constant motion. Weather changes every season because of the earth's tilt when it revolves around the Sun. Some determining factors of weather are temperature, precipitation, fronts, clouds, and wind. Other more severe conditions are hurricanes, tornadoes, and thunderstorms. Clouds and storms form when pockets of air rise and cool.

The conditions in the troposphere have a profound effect on the propagation of radio waves as we will explain later.

1.1.2 Stratosphere



Figure 1.4 A picture, taken from an airplane, of stratospheric clouds.

The atmosphere, above the tropopause, 10 km up to 50 km altitude is called the stratosphere. In this layer, the temperature basically increases again with altitude up to a local maximum, which defines its top boundary, stratopause.

Many jet aircrafts fly in the stratosphere because it is very stable. The gas is still dense enough that hot air balloons can ascend to altitudes of 15-20 km and Helium balloons to nearly 35km.

The **ozone layer** exists in the stratosphere. The ozone molecules absorb dangerous kinds of sunlight, which heats the air around them. On Earth, ozone causes the increasing temperature in the stratosphere.

Because it is a relatively calm region with little or no temperature change, the stratosphere has almost no effect on radio waves.

1.1 3 Mesosphere



Figure 1. 5. This is an image which shows the Earth and its atmosphere from space.
The mesosphere would be the dark blue edge on the far right hand side.

The next layer on top of the stratosphere between 30 and 80 km above msl is called mesosphere. T (see Fig.1.5). In the Earth's mesosphere, the air is relatively mixed together. The temperature drops again to local minimum at its upper boundary, in the mesopause. The atmosphere reaches its coldest temperature of around -90°C in the mesosphere.

While entering the Earth's atmosphere, a lot of meteors or rock fragments burn up near and below the mesopause where meteors typically can be seen streaking across the sky.

1.1 4. Thermosphere



Figure 1.6 This is an image of the space shuttle as it is orbiting around the Earth.

It is the region of Earth's upper atmosphere extending up to 500 km. It is also where the space shuttle orbits. In this region, the atmospheric temperature first increases with altitude to an overall maximum value (~1000 K) and then becomes constant with altitude. The air is really thin in the thermosphere. Also, photo-dissociation of the dominant N₂ and O₂ molecules is important and acts to produce copious amounts of O and N atoms. The thermosphere is a layer with auroras. The Earth's thermosphere also includes the region of the atmosphere called ionosphere. The ionosphere is the ionized portion of the upper atmosphere.

1.1 5 Exosphere



Figure 1.7 A picture which shows the Earth's atmosphere. The clouds are likely in the troposphere and stratosphere, the dark blue curve/edge is the mesosphere and thermosphere and the dark blue to black region of space where our exosphere extends out.

At about 500 km, the neutral densities become so low that collisions become unimportant and hence the upper atmosphere can no longer be characterized as fluid. This transition altitude is called the exobase, and the region above it is called the exosphere.

1.2 IONOSPHERE

The ionosphere extends from 60 km to 2000 km altitude. Because the composition of the atmosphere changes with height, the ion production rate also changes and this leads to the formation of several distinct ionization peaks, the "D" (50 km to 90 km), "E" (90 km to 120 km), "F" layers above the surface of the Earth.

Different regions of the ionosphere make long distance, point-to-point radio communications possible by reflecting the radio waves back to Earth.

1.2.1 Ionospheric Layers

D-LAYER

- The dominant ions are NO^+ and O_2^+ .
- Ionization here is due to Lyman series-alpha hydrogen radiation at a wavelength of 121.5 nanometre (nm) ionizing nitric oxide (NO).
- The D layer is mainly responsible for absorption of HF radio waves, particularly at 10 MHz and below, with progressively smaller absorption as the frequency gets higher.
- The absorption is small at night and greatest about midday.
- The layer reduces greatly after sunset, but remains due to galactic cosmic rays. A common example of the D layer in action is the disappearance of distant AM broadcast band stations in the daytime.

E-LAYER

- The dominant ions are NO^+ and O_2^+ .
- Ionization is due to soft X-ray (1-10 nm) and far ultraviolet (UV) solar radiation ionization of molecular oxygen (O_2).
- This layer can only reflect radio waves having frequencies less than about 10 MHz.
- At night the E layer begins to disappear because the primary source of ionization is no longer present.

- The increase in the height of the E layer maximum increases the range to which radio waves can travel by reflection from the layer.
- The E region peaks at about 105km.

E_s-LAYER

- Es or Sporadic E propagation is characterized by small clouds of intense ionization, which can support radio wave reflections from 25 – 225 MHz.
- Sporadic-E events may last for just a few minutes to several hours and make radio amateurs very excited, as propagation paths which are generally unreachable, can open up.
- This propagation occurs most frequently during the summer months with major occurrences during the summer, and minor occurrences during the winter.
- During the summer, this mode is popular due to its high signal levels.

F-LAYER

- In the F region O⁺ ion dominates.
- Above the F region is a region of exponentially decreasing density known as the "topside ionosphere." This region extends to an altitude of a few thousand kilometers.
- Here extreme ultraviolet (UV) (10-100 nm) solar radiation ionizes atomic oxygen (O).
- The F region is the most important part of the ionosphere in terms of HF communications.
- During daytime, it divides into two layers, the F1 and F2.
- The F layers are thickest and most reflective of radio on the side of the Earth facing the sun.

On a more practical note, the D and E regions reflect AM radio waves back to Earth. Visible light, television and FM wavelengths are all too short to be reflected by the ionosphere. So your tv. stations are made possible by satellite transmissions.

1.2 2 Ionospheric density profile

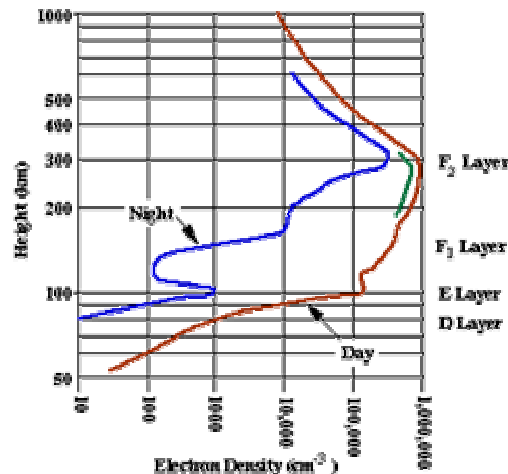


Figure 1.11 The densities and locations of ionospheric layers are shown for both night and day conditions at mid-latitudes.

Plasma densities in the ionosphere are characterized by strong day-night variability. Ionospheric plasma densities also vary markedly with season, solar cycle, and level of geomagnetic activity.

1.2.3 Aurora

When protons and electrons from the Sun travel along the Earth's magnetic field lines above the north and south poles there is an oval region charged particles can enter the ionosphere and excite its neutral atoms and molecules, giving off light , just like florescent lighting.



This all happens in the ionosphere, 60-200 km up. We are talking major-league energy, much more than the power of lightning: 20 million amps at 50,000 volts is channeled into the auroral oval. The aurora is also known as the northern and southern lights. Sometimes, when the Sun is active, the northern auroral oval expands and the aurora can be seen much farther south.

CHAPTER 2:

THE TERRESTRIAL-IONOSPHERE AT HIGH LATITUDES

2.1.ELECTROMAGNETIC COUPLING

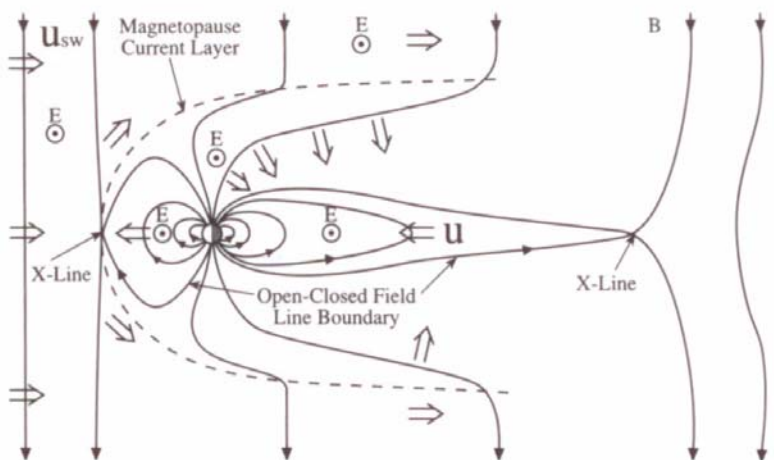


Figure 2.1 Schematic diagram showing the direction of the electricity and magnetic fields, and plasma flows , in the vicinity of Earth. The Sun also is to the left, north is the top, south is at the bottom.

Electromagnetic coupling is perhaps the most process linking the magnetosphere-ionosphere and thermosphere at high latitudes. The coupling arises as a result of the interaction of themagnetized solar wind with the Earth's geomagnetic field. When the supersonic solar wind first encounters the geomagnetic field, a free-standing bow shock is formed that deflects the solar wind around the Earth in a region called the magnetosheath. The subsequent interaction of the magnetosheath flow with the geomagnetic field leads to the formation of the magnetopause, which is a relatively thin boundary layer that acts to separate the solar wind's magnetic field from the geomagnetic field. The separation accomplished via magnetopause current system.

However, the shielding is not perfect, and a portion of the solar wind's magnetic field (also known as the interplanetary magnetic field) penetrates the magnetopause and connects with the geomagnetic field. This connection is shown in Fig.3.2 for the case of southward IMF. Note that the IMF has components in the ecliptic plane directed along the Sun-Earth line(positive toward the sun) in the ecliptic plane directed perpendicular to the Sun-Earth line (positive toward the dusk) the north-south component perpendicular to

the ecliptic plane (positive toward the north). The connection of the IMF and the geomagnetic field occurs in a circular region known as the polar cap, and the connected field lines are referred to as open field lines. The auroral oval is an intermediate region that lies between the open line region (polar region) and the low-latitude region that contains dipolar magnetic field lines. The field lines in the auroral oval are closed, but they are stretched deep in the magnetospheric tail.

2.2 CONVECTION ELECTRIC FIELDS

The solar wind is a highly conducting, collisionless, magnetized plasma that, to lower, can be derived by ideal MHD equations. Therefore, the electric field in the solar wind is governed by the relation $\mathbf{E} = -\mathbf{u}_{sw}\times\mathbf{B}$, where \mathbf{u}_{sw} is the velocity of solar wind. When the radial solar wind, with a southward IMF component interacts with the Earth's magnetic field (Fig.3.2), an electric field is imposed that points in the down-to-dusk direction across the polar cap. This imposed electric field, which is directed perpendicular to \mathbf{B} , maps down to the ionospheric altitudes along highly conducting geomagnetic field lines. In the ionosphere, this electric field causes the plasma in the polar cap to \mathbf{ExB} drift in an antisunward direction. Further, from the Earth, the plasma on the open polar cap field lines exhibits an \mathbf{ExB} drift that is toward the equatorial plane. In the distant magnetospheric tail, the field lines reconnect, and the flown on those closed field lines is toward and around the Earth. The existence of an electric field across the polar cap implies that the boundary between open and closed magnetic field lines is charged. The charge is positive on the dawnside and negative on the duskside, as shown in the solar wind out of the plane of the Fig.3.2 and earth is at the top.

The charges on the polar cap boundary act to induce electric fields on nearby closed field lines that are opposite to in direction to the electric fields in the polar cap. These oppositely directed electric fields are situated in the regions just equatorward of the dawn and dusk sides of the polar cap. As with the polar cap electric field, the electric fields on the closed field lines map down to the ionospereic altitudes and cause the plasma to \mathbf{ExB} drift in a sunward direction. On the field lines that separate the oppositely directed fields, field-aligned (or Birkeland) currents flow between the ionosphere and magnetosphere. The current flow is along \mathbf{B} and toward the ionosphere on the dawnside, across \mathbf{B} and away from the ionospere on the duskside.

The net effect of the electric configurationin Fig.3.2 is as follows. Closed dipolar magnetic field lines connect to the IMF at the dayside magnetopause. When this connection occurs, the ionospheric foot of the field line is at the dayside boundary of the polar cap. After connection, the open field line and attached plasma, convect in an antisunward direction across the polar cap. When the ionospheric foot of the open field line is at the nightside polar cap boundary, the magnetospheric end is in equatorial plane of the distant magnetotail.

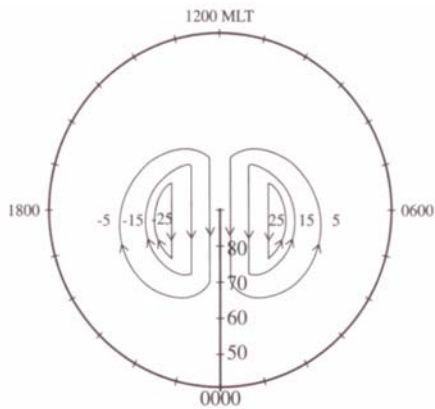


Figure 2.2 Contours of magnetospheric electrostatic potential in a magnetic latitude MLT reference frame. The contours display a 2-cell pattern.

The open field line then reconnects, and subsequently, the newly closed and stretched field line convects around the polar cap and toward the dayside magnetopause. The direction of the $\mathbf{E} \times \mathbf{B}$ drift in the ionosphere that is associated with the magnetospheric electric field shown in Fig.3.4. Magnetospheric electric fields are not the only source of ionospheric drift and, therefore, it is important to determine the relative contributions of the various sources. The net electrodynamic drift is driven by both magnetospheric and corotational electric fields. The ionosphere at low and middle altitudes is observed to corotate with the Earth, and this motion is driven by a corotational electric field.

At high latitudes, the plasma also has a tendency to corotate, and this must be taken into account when calculating the plasma convection paths. The corotational electric field causes the plasma to drift around the Earth once every 24 hours and, as a consequence, the plasma remains above the same geographic pole at the center the drift trajectories are concentric circles about the geographic pole. Because the offset is 11.50 in the northern hemisphere and 14.50 in the southern hemisphere.

For magnetic convection, assuming to be the magnetic pole at the center and the noon-midnight direction taken as one of the axes, the magnetospheric convection pattern stays aligned with the noon-midnight axis as the magnetic pole rotates about the geographic pole. As it turns out, corotation in the **geographic inertial frame** is equivalent to corotation in this **magnetic inertial frame**.

2.2.1 Convection Models

The empirical convection models represent average magnetospheric conditions, not instantaneous patterns. Convection boundaries that exist in these models more smoothly, whereas the instantaneous convection boundaries can be fairly sharp. When the IMF is southward plasma convection at high latitudes exhibits a 2-cell pattern with antisunward flow over the polar and return flow equatorward of the polar cap. For southward IMF, a new empirical model of magnetospheric electric fields for plasma

convection constructed from a large database of satellite measurements yields multi-cell convection pattern for northward.

2.2.2 Effects of Convection Model

The effect that convect ion electric field have on the ionosphere depends on altitude. At ionospheric altitudes, the electron-neutral collision frequency is much smaller than the electron cyclotron frequency and hence , only the combined effect of the perpendicular electric field ,**E**, and the geomagnetic field, **B**, is to induce and electric drift in the **ExB** direction. For ion, the ion-neutral colision frequencies are greater than the corresponding cyclotron frequencies at E-region, with the result that the ion drift in the direction of the perpendiculaar electric field. Since the ion-neutral frequency decreases as the altidute increases,at F-region altitudes both ions and electron drifts in the **ExB** direction.

At altitude above 800 km, the plasma begin to flow ouT ofthe topside ionosphere with a speed that increases with altitude, and this phenomena is known as polar wind. The neutral wind vectors are consistent with 2-cellplasma convection pattern, which occurs when the IMF is southwad. When the IMF is northward, multi-cell signature should also be reflected in the thermosphere circulation pattern. The ions are frictionally heated via ion-neutral collisions, as they convect through the slower moving neutral gas, and this acts to raise the ion temperature.

2.3 PARTICLE PRECIPITATION

Energetic electron precipitation in the auroral oval not onlyis the source of optical emision, but also, is a source of ionization due to electron impact with the neutral atmosphere,

A source of bulk heating for both ionosphere and atmosphere,

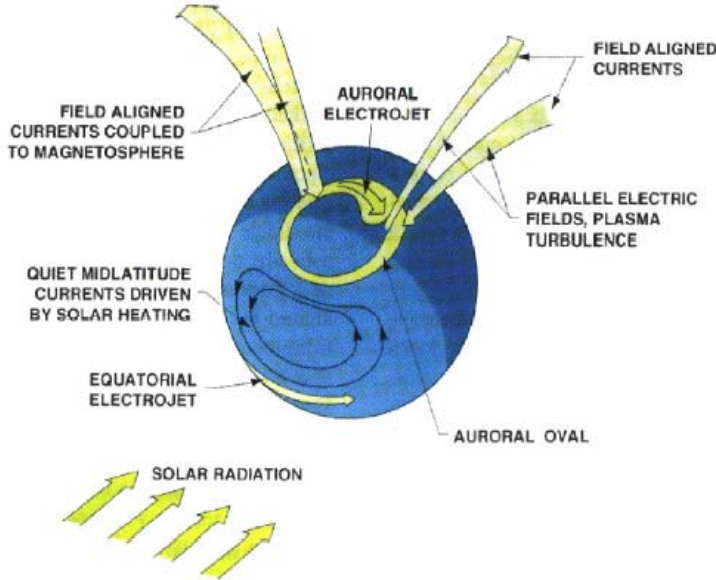
A source of heat that flows down from the lower magnetosphere into the iosphere

For a southward IMF, the electron precipitaiton occurs in distinct regions in the aurora; diffusive auroral precipitation, discrete arcs in the nocturnal oval, low energy polar rain precipitation, soft precipitation in the cusp and diffusive auroral patches in the morning oval.

For a northward IMF, there are sun-aligned arcs in the polar cap. Ion precipitation also occurs in the auroralzone and, on average, the ion precipitation pattern varies systematically with magnetic latidute, magnetic local time, and Kp.

The average energy of the percipitating ions is substantially greater than than that for the precipitating electrons. For quiet magnetic conditions the maximum energy flux is about 1 erg cm -2 s^{-1} . For active conditions, the maximum energy flux reaches 8 ergcm -2 s^{-1} . In general, the particle precipitation in the auroral zone is structured and highly time dependent.

2.4 CURRENT SYSTEMS



The precipitation auroral electrons are responsible for the upward field-aligned (Birkeland) currents (Region 1 currents). They flow in the ionosphere in the morning sector and away from the ionosphere in the evening sector. Associated with these precipitating magnetospheric electrons there are upflowing ionospheric electrons, which provide for a return current.,i.e., downward field-aligned current. They flow in the opposite direction to the previous one (Regio 2 currents).

Also, the cusp field-aligned currents are located poleward of the upward and down field-aligned currents.(not shown in figure.)and generally emerge flow away from the ionosphere in the prenoon sector and into the ionosphere in the postnooon sector.

When the IMF is nowrdward, the NBZ currents are concentrated on the sunlit side of the polar cap. They are poleward of the Region 1 currents and opposite direction to them. When the NBZ currents exist Region 1 and Regin 2 currents continue to exist. In the southern hemisphere, the NBZ currents flow into ionosphere on the duskside of the polar cap and away from the ionospher on the dawsid. The field-aligned current are connected via horizontal currents which are the large scale current flowing in the lower ionosphere.

S_q ionospheric currents are resulted from tidal winds and **Equatorial electrojet** is concentration of S_q around the equator. **Auroral electrojet:** are Hall currents fed by field-aligned currents from the magnetosphere and associated with auroral activity.

2.5 LARGE SCALE IONOSPHERIC STRUCTURES

The magnetospheric electric fields, particle precipitation, and field-aligned currents act in concert to produce large-scale ionospheric structures. These include

- Polar holes,
- Ionization troughs,
- Tongues of ionization,
- Plasma patches,
- Auroral ionization enhancements, and
- Electron and ion temperature hot spots.

Whether a feature occurs and the detailed characteristics of a feature depend on the phase of the solar cycle, season, time of day (diurnal) type of convection pattern, and the strength of convection.

Most of the large-scale features that have been identified occur for southward IMF. In this case, 2-cell convection pattern exists, with anti-sunward flow over the polar cap and sunward at lower altitudes. The effect of the anti-sunward flow is to transport the high density dayside plasma into the polar cap. The **polar hole** is a region on the nightside of the polar cap where reduced ionization exists because of the long transport time of ionization from the dayside across the polar cap. In summer, when the bulk of the polar cap is sunlit, difference in anti-sunward convection is not significant since the plasma density tends to be uniform. In winter, it is important. In the auroral oval, the density is enhanced because of the impact ionization due to precipitating electrons.

The net result is a polar hole if the antisunward convection speed is low and it situated just poleward of the nocturnal oval. When the speed is high, high-density dayside plasma can be transported great distances before it decays appreciably. The net result is a **tongue of ionization** extending across the polar cap from the dayside to the nightside. **Main or mid-altitude electron density trough** which is located equatorward of the nocturnal auroral oval is a region of low electron density that has a narrow latitudinal extent, it is extended in longitude. **Ion temperature hot spots** can occur in the high-latitude ionosphere during periods when the convection electric fields are strong and near the dusk and/or dawn meridians. **Electron temperature hot spots** exist in high-latitude ionosphere due to mainly electron precipitation.

Plasma patches are created either in the dayside cusp or just equatorward of the cusp. Their densities are a factor of 3-10 greater than the background densities and their horizontal dimensions vary from 200 to 1000 km

Sun-aligned polar cap arcs appear when the IMF is near zero or northward and as a result of electron precipitation, with characteristic energy varying from 300 eV to 5 keV. They are relatively narrow (< or = 300 km) across polar cap, but extended along noon-midnight direction (1000-3000 km).

2.6 GEOMAGNETIC STORMS

A geomagnetic storm is a temporary intense disturbance of the Earth's magnetosphere. when there is a sudden change in the solar wind dynamic pressure at magnetopause. It occurs when it is impacted by a coronal mass ejection or solar flare material . There subsequent propagation toward lower latitude leads to a travelling ionospheric disturbance.

2.7 SUBSTORMS

At mid-latitudes, the equatorward propagating waves drive the F region ionization toward higher altitude which result in ionization enhancement. Associated with substorms are localized regions of enhanced electric fields, particle precipitation, and both field-aligned and electrojet currents.

2.8 POLAR WIND

The classical polar wind is and amipolar outflow of thermal plasma from the high-latitude ionosphere As the light ion plasma flows up and out of the topside ionosphere along diverging geomagnetic field lines, it undergoes four major transitions,

- A transition from chemical to diffusion dominance
- A transition from the subsonic to supersonic flow,
- A transition from collision-dominted to collissionless regimes, and
- A transition from a heavy (O^+) to a light (H^+) ion

At times,hower, O^+ can remain the dominant ion to very high altitudes in the polar cap.

CHAPTER 3:

PHYSICS

OF

THE NEUTRAL ATMOSPHERE

Altitude [km]	Temperature	Ionization	Magnetic field	Propagation	Technical
10000	Thermosphere	Protonosphere		Ionosphere	Upper Atmosphere
1000		Ionosphere	Magnetosphere		
100	Mesosphere				
10	Stratosphere		Dynamosphere		Lower Atmosphere
	Troposphere	Neutrosphere		Troposphere	

Figure 3.1 Possible subdivision schemes of the earth's atmosphere , after (Seeber, 1993).

3.1 PHYSICS LAWS FOR THE NEUTRAL ATMOSPHERE

Characterizing the atmosphere by the radio waves are propagated leads to a subdivision troposphere and ionosphere. The ionosphere, the upper part of the atmosphere, is the dispersive medium (the propagation delay is frequency dependent) whereas the troposphere is non-dispersive. The troposphere is also referred to as neutral atmosphere.

In this chapter the following physical laws and equations are given the gas equation (equation of state), hydrostatic equation, and Snell's law

3.1.1 .Equation of state

In (Champion,1960) three laws for gases are given:

Charles' constant pressure law:

“ At constant pressure for a rise in temperature of 1degree Celsius, all gases expand by a constant amount, equal to 1/ 273 of their volume at 0 degree Celsius”.

Charles' constant volume law:

“ If the volume is kept constant, all gases undergo an increase in pressure equal to 1/ 273 of their pressure at 0 degree Celsius”.

Boyle's law :

“ At constant temperature the product of pressure and volume is constant” .

- Based on these laws, the gas equation of state is formulated for perfect gases:

$$\alpha P = R_i T \quad (3.1)$$

with

α : specific volume $[m^3 kg^{-2}]$

P : pressure $[N m^{-2}]$

R_i : specific gas constant $[J kg^{-1} K^{-1}]$

T : temperature $[K]$

$[N] : [kg m s^{-2}]$

$[J] : [Nm]$

The specific volume α is defined as :

$$\alpha = \frac{1}{\rho} = \frac{V}{m} \quad (3.2)$$

with

ρ : density $[kg m^{-3}]$

V : volume $[m^3]$

m : mass $[kg]$

The specific gas constant R_i (for the i^{th} gas) is related to the universal gas constant by :

$$R_i M_i = R \quad (3.3)$$

with

$$M_i : (\text{mean}) \text{molecular mass} [\text{kg mol}^{-1}]$$

$$R : \text{universal gasconst.} [8.31434 \text{ J mol}^{-1} \text{ K}^{-1}]$$

Although there is no perfect gases, the gas in the troposphere are nearly perfect and can often be treated as such. as

The equation of state does not only hold for one specific gas, but also a mixture of gases. In that case,

P is the sum of the particle pressures,

R_i is the specific gas constant of the mixture, and

M_i is the mean molecular mass of the mixture.

3.1.2 Hydrostatic equilibrium

The atmosphere is said to be in hydrostatic equilibrium if the vertical forces on any slice of a column of air with thickness dh is equal to zero (Haltiner and Martin, 1957).

If one thinks of a slice with unit area, the vertical forces can be expressde in terms of pressure(force per unit area).

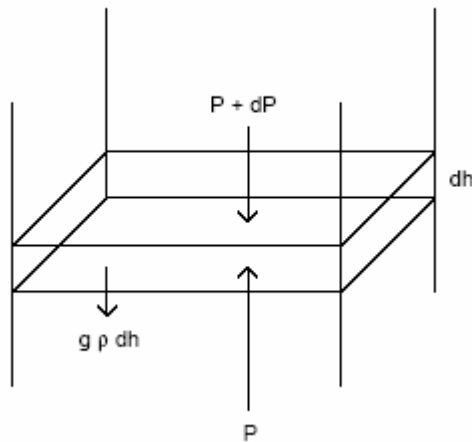


Figure 3.2 Vertical forces on a unit slice of thickness dh in hydrostatic equilibrium

The downward force is equal to the force at the top of the slice $P+dP$ plus force due to gravity $g h dh$; see Fig.4.2. The upward force is equal to the pressure at the bottom of the slice P .The hydrostatic equation therefore reads:

$$g \rho dh + (P + dP) = P \quad (3.4)$$

Rewriting Eq.(3.4) gives:

$$dP = -gPdh \quad \text{or} \quad \frac{dP}{dh} = -gP, \quad (3.5)$$

with

g : gravitational acceleration $[ms^{-2}]$
 h : height above msl (mean sea level)

Using the definition of Eq.(2), this may be also written as:

$$gh = -\alpha P \quad (3.6)$$

3.1.3 Snell's law

A radio signal passing through the Earth's atmosphere suffers a change in direction owing to refraction. If we consider the neutral atmosphere to be horizontally stratified and neglect the ionospheric refraction, the total bending can be found by repeatedly applying Snell's law for each layer (Smart, 1936).

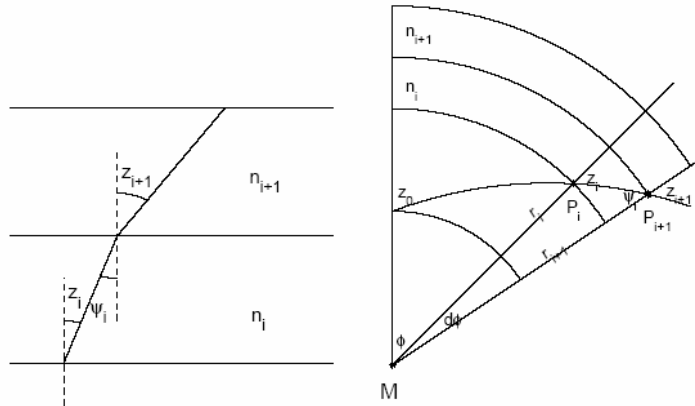


Figure 3.3 Illustration of Snell's law in cartesian coordinates(left side) and snell's law in spherical coordinates (right side) for horizontally stratified layers z_i ; zenith angle of layer i ; n_i refractive index of layer i .

Snell's law states (see Fig.3.3):

$$n_{i+1} \sin z_{i+1} = n_i \sin z_i = n_i \sin \psi_i \quad (3.7)$$

where z_i and z_{i+1} are the zenith angle of the arriving radio signal in the layer i and $i+1$, n_i and n_{i+1} are the corresponding refractive indexes.

By applying the Snell's law for each layer, one finds:

$$n_0 \sin z_0 = \sin z_m \quad (3.8)$$

where the index i denotes the lowest layer and the index n_0 denotes the highest layer, where the refractive index reduces to 1. This formula holds for any refractivity profile.

For a spherical Earth we may formulate Snell's law in spherical coordinates (Smart, 1936). Application of sine rule in the triangle MP_iP_{i+1} of Fig.4.2 gives:

$$\frac{r_i}{\sin \psi_i} = \frac{r_{i+1}}{\sin(\pi - z_i)} = \frac{r_{i+1}}{\sin z_i} \quad (3.9)$$

where r_i and r_{i+1} are the distances MP_i and MP_{i+1} with M two center of mass of the Earth. Combining Eq.(7) and (9) gives Snell's law in spherical coordinates:

$$n_{i+1}r_{i+1} \sin z_{i+1} = n_i r_i \sin z_i = n_0 r_0 \sin z_0 \quad (3.10)$$

or simply

$$n_0 \sin z_0 = \sin z_m \quad (3.11)$$

3.2 WATER VAPOR

The troposphere contains both dry air and water vapor. Dry air has no significant variation in composition with altitude and height (Smith and Weintraub, 1953). The amount of water vapor, on the other hand, varies widely, both spatially and temporally.

Water also appears in the troposphere in liquid phase (fog, clouds, rain) and solid form (snow, hail, ice) and is the most important constituent in relation to weather processes, not only because of rain- and snowfall but also because large amounts of energy are released in condensation process.

In this section, we deal with some water-vapor related measures like mixing ratio, partial pressure of vapor, relative humidity

3.2.1 Mixing ratio

The mixture of dry air and water vapor is called **moist air**. A measure of moisture air is the **mixture ratio**, which is defined as the quotient of water-vapor mass per unit mass dry air (Haltiner and Martin, 1957).

$$w = \frac{m_v}{m_d} = \frac{m_v/V}{m_d/V} = \frac{\rho_v}{\rho_d} \quad (3.12)$$

w : mixing ratio [-]

m_v : mass of water vapor [kg]

m_d : mass of dry air [kg]

V : volume $[m_3]$

ρ_v : density of water vapor $[kg\ m^{-3}]$

ρ_d : density of dry air $[kg\ m^{-3}]$

If we apply the equation of state, Eq.(3.1), for both water vapor and dry air, we obtain with use of Eq.(3.13):

$$e = \rho_v R_v T; \quad P_d = P - e = \rho_d R_d T \quad (3.13)$$

where

e : partial pressure of water vapor $[Nm^{-2}]$

P_d : particle pressure of dry air $[Nm^{-2}]$

P : total pressure of (moist air) $[Nm^{-2}]$

R_v : specific gas constant of water vapor $[J\ kg^{-1}\ K^{-1}]$

R_d : specific gas constant of dry air $[J\ kg^{-1}\ K^{-1}]$

Another expression for the mixing ratio can be obtained from Eq.(4.12) and (4.13):

$$w = \frac{e/R_v T}{(P-e)/R_d T} \quad (3.14)$$

$$R_d = 237.06 \pm 0.01 \ J\ kg^{-1}\ K^{-1}$$

$$R_v = 461.525 \pm 0.003 \ J\ kg^{-1}\ K^{-1}$$

$$\epsilon = \frac{R_d}{R_v} = 0.622$$

The approximation is allowed because the partial pressure of water vapor is typically about 1% of the total pressure. The constant in Eq.(3.14) are taken from (Mendes, 1999). An alternative to express the humidity is the **specific humidity**

:

$$q = \frac{\rho_0}{\rho_m} \approx w \quad (3.15)$$

3.2.2 Virtual temperature

We can also apply the equation of state for moist air. In that case we have :

$$P = \rho_m R_m T, \quad (3.16)$$

ρ_m : density of moist air $[kg\ m^{-3}]$

R_m : specific gas constant of moist air $[J kg^{-1} K^{-1}]$

Since $\rho_m = \rho_v + \rho_d$, combining Eq.(12), Eq.(13), and Eq.(16) gives R_m as a function of the mixing air:

$$R_m = \frac{R_d + w R_v}{1+w} = \frac{R_d(1+1.16w)}{1+w} \approx R_d(1+0.61w) \quad (3.17)$$

Substituting Eq.(4.17) in Eq.(4.16)

$$P = \rho_m R_m T_v, \quad (3.18)$$

where

$$T_v = (1+0.61w)T, \quad (3.19)$$

is the **virtual temperature** in kelvin.

In Eq.(3.18) the fixed gas constant R_d is used instead of R_m . The virtual temperature is accounted for by the use of a fictitious temperature.

3.2.3 Partial pressure of saturated air

In a closed system with no air, an equilibrium will be established when equal number of water molecules are passing from liquid or solid to vapor, and vice versa. Under these circumstances the vapor is said to be **saturated**. When the vapor is mixed with air, the mixture of air and water vapor under equilibrium conditions is referred to as a saturated air. When saturated air comes in contact with unsaturated air, **diffusion** takes place in the direction toward lower values of vapor.

The partial pressure of saturated water vapor is a function of temperature. Larger amounts of water vapor can be contained by warmer air. By cooling saturated air, the surplus of water vapor above the saturation value at the new temperature condenses. The energy released (per unit mass) in the condensation is called **latent heat**. The same amount of energy is required for vaporization. We also have the latent heat of fusion, which is the amount of energy required in the change of a unit mass of ice to liquid water, the latent heat of sublimation, which is the sum of the latent heats of vaporization and fusion.

A relation between latent heat, partial pressure of water vapor and temperature, is given by the **Clausius-Clapeyron equation** (Haltiner and Martin, 1957):

$$\frac{1}{e_{sat}} = \frac{de_{sat}}{dT} = \frac{L}{R_v T^2} \quad (3.20)$$

e_{sat} : partial pressure of saturated water vapor $[N m^{-2}]$

L : latent heat of fusion $[0.334 \cdot 10^6 \text{ J kg}^{-1}]$ or
 latent heat of vaporization $[2.500 \cdot 10^6 \text{ J kg}^{-1}]$ or
 latent heat of sublimation $[2.834 \cdot 10^6]$
 R_v : specific gas constant of water vapor $[461.525 \text{ J kg}^{-1} \text{ K}^{-2}]$

In integration of Eq.4.(20) gives the partial pressure of water vapor as a function of temperature:

$$e_{sat} = e_{sat}(0) \exp \left[-\frac{L}{R_v} \left(\frac{1}{T} - \frac{1}{T(0)} \right) \right], \quad (3.21)$$

with L either the latent heat of vaporization ($T > 0^\circ \text{C}$) or sublimation ($T < 0^\circ \text{C}$) The integration constants are given at 0°C

$$e_{sat}(0) = 6.11 \text{ mbar} \equiv 611 \text{ Nm}^{-2}; \\ T(0) = 273.16 \text{ K}$$

The Clausis-Clapeyron equation is a theoretical model. Slightly different values are derived by (Baby et al.,1988) using (Quency,1974):

$$e_{sat} = \exp \left[A - \frac{B}{T} \right]; \quad (3.22)$$

$$A = 21.3195 \text{ and } B = 5327.1157 \text{ K for } T < T(0)$$

$$A = 24.3702 \text{ and } B = 6162.3496 \text{ K for } T > T(0)$$

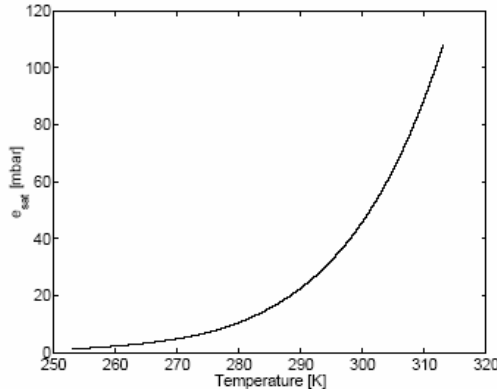


Figure 3.4 Partial pressure of saturated air according to (Baby et al.1988).

This expansion is similar to Eq.(21) and is shown graphically in Fig.4.4. We may also define a saturation mixing ratio;cf Eq.(14). This is given as (Haltiner and Martin, 1957);

$$w_{sat} = \frac{e_{sat}}{P - e_{sat}} \approx \frac{e_{sat}}{P}, \quad (3.23)$$

w_{sat} : saturation mixing ratio [-]

3.2.4 Relative Humidity

The relative humidity

is defined as the quotient the mixing ratio and saturation mixing ratio:

$$r_h = \frac{w}{w_{sat}} \approx \frac{e}{e_{sat}} \quad (3.24)$$

r_h : relative humidity [−]

The relative humidity is often multiplied by hundred to express it in percentages.

3.3 PROPAGATION DELAY AND REFRACTIVITY

The total delay of a radio signal caused by the neutral atmosphere depends on the refractivity along the travelled path, and The refractivity depends on pressure and temperature The basic physical law for propagation is **Fermat's principle**:

"Light (or any electromagnetic wave) will follow the path between two points involving the least travel time".

We define the electromagnetic (or optical) distance between source and receiver as:

$$S = \int t dt = \int \frac{c}{v} ds = \int n(s) ds, \quad (3.25)$$

where

S : electromagnetic distance [m]

s : electromagnetic path [m]

c : speed of light in vacuum [$m s^{-1}$]

$v = \frac{ds}{dl}$; propagation speed [$m s^{-1}$]

$n = \frac{c}{v}$; refraction index [−]

The excess path length becomes

$$D_t^s = S - L = \int_s^l (n(s) - 1) ds + \left\{ \int_s^l ds - \int_l^l dl \right\} \quad (3.27)$$

Where D_t^s excess path length in the slant direction caused by troposphere [m].

The first term on the right-hand side is the excess path length caused by the propagation delay, Whereas the second term (between braces) is the excess path length caused by bending. From now on we will just speak of delay, instead of excess path length:

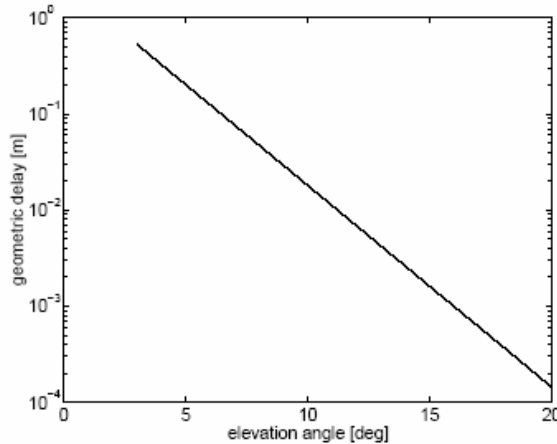


Figure 3.5 Delay caused by ray bending ; model by (Mendes, 1999)

So when we speak of a delay, it is in terms of distance. In (Mendes,1999) a model (called dg.V1) is given for the delay caused by the bending based on ray tracking results

$$\alpha \exp(-\varepsilon/b) \text{ with } a = 2.256 \pm 0.0092 \text{ m},$$

$$b = 2.072 \pm 0.0054^\circ,$$

ε the elevation angle, see Fig.5

Because the value of the refractive index is close to 1, often the refractivity N (Neper) is used:

$$N = (n - 1) \cdot 10^6 \quad (3.28)$$

Values for N in the ionosphere range between 0 and 300. Since the neutral atmosphere contains both dry air and water vapor, the refractivity can also be split into a dry and a vapor part (Smith and Weintraub,1953):

$$N = N_d + N_v \quad (3.29)$$

N_d : refractivity of dry air [-]

N_v : refractivity of water vapor [-]

This makes sense because the mixing ratio of dry-air constituents remains nearly constant in time. While the water-vapor content fluctuates widely, both spatially and temporally.

According to(Tayer,1974), for frequencies up to 20 GHz we may write the refractivities as a function of temperature and partial pressures:

$$N_d = k_1 \frac{P_d}{T} Z_d^{-1};$$

$$N_v = \left[k_2 \frac{e}{T} + k_3 \frac{e}{T^2} \right] Z_v^{-1}$$
(3.30)

k_i : constants [K mbar^{-1} for $i=1,2$; $\text{K}^2 \text{mbar}^{-1}$ for $i=3$]

Z_d : compressibility factor of dry air [-]

Z_v : compressibility factor of water vapor [-]

The constants have been determined empirically. Different values are given in Table 3.1.

Reference	k_1 [K mbar $^{-1}$]	k_2 [K mbar $^{-1}$]	k_3 $10^5 [\text{K}^2 \text{mbar}^{-1}]$	k'_2 [K mbar $^{-1}$]
[Boudouris, 1963]	77.59 ± 0.08	72 ± 11	3.75 ± 0.03	24 ± 11
[Smith and Weintraub, 1953]	77.61 ± 0.01	72 ± 9	3.75 ± 0.03	24 ± 9
[Thayer, 1974]	77.60 ± 0.01	64.79 ± 0.08	3.776 ± 0.004	17 ± 10

Table 3.1

The dry refractivity and the first term of the vapor refractivity represents the effects of the permanent dipole moment of the water vapor molecule (Thayer;1974). The inverse compressibility factors are given by the empirical formulas (Owens,1967):

$$Z_d^{-1} = 1 + P_e \left[57.90 \cdot 10^{-8} - 9.4581 \cdot 10^{-4} T^{-1} + 0.25844 T^{-2} \right]$$

$$Z_v^{-1} = 1 + e \left[1 + (3.7 \cdot 10^{-4}) e \right]$$

$$\left[-2.37321 \cdot 10^{-3} + 2.3366 T^{-1} - 710.792 T^{-2} + 7.75141 \cdot 10^4 T^{-3} \right]$$

These factors account for the nonideal behavior of dry air and water vapor. Under normal circumstances these are close to unity. With these compressibility factors the general equation of state becomes:

$$P_i = Z_i \rho_i R_i T,$$
(3.32)

P_i : partial pressure of the i^{th} constituent [Nm^{-2}]

ρ_i : mass density of the i^{th} constituent [kgm^{-3}]

R_i : specific gas constant of the i^{th} constituent [$\text{J kg}^{-1} \text{K}^{-1}$]

Often, dry air and water vapor are considered to be ideal gases with unit compressibility factors:

$$N_d : k_1 \frac{P_d}{T};$$
(3.33)

$$N_v : k_2 \frac{e}{T} + k_3 \frac{e}{T^2}.$$

Instead of splitting the refractivity into dry and a vapor part, we can also split into a hydrostatic and non-hydrostatic part (Davis et al., 1985).

With Eq.(3.30) and the equation of state for dry air and water vapor ($i=d,v$) becomes:

$$\begin{aligned} N &= k_1 R_d \rho_d + k_2 R_v \rho_v + k_3 \frac{e}{T^2} Z_v^{-1} \\ &= k_1 R_d \rho_m - k_1 R_d \rho_v + k_2 R_v \rho_d + k_3 \frac{e}{T^2} Z_v^{-1} \\ &= k_1 R_d \rho_m + \left(k_2 - k_1 \frac{R_d}{R_v} \right) R_v \rho_v + k_3 \frac{e}{T^2} Z_v^{-1} \end{aligned} \quad (3.34)$$

where we used the density of moist air $\rho_m = \rho_d \rho_v$. If we define

$$\begin{aligned} k'_2 &= k_2 - k_1 \frac{R_d}{R_v} = k_2 - k_1 \in \\ k_2 &: \text{constant} \left[K^{-1} mbar^{-1} \right] \end{aligned} \quad (3.35)$$

and use the equation of state for water vapor.

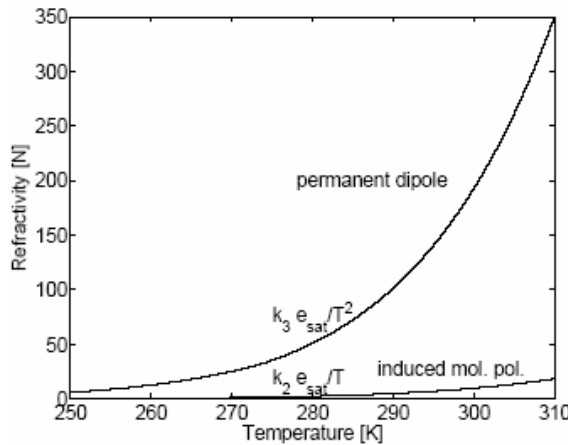


Figure 3.6 Contribution of both parts of the wet refractivity for saturation pressures; k_1, k_2 , according to (Thayer, 1974)

Eq.(3.34) becomes:

$$\begin{aligned} N &= k_1 R_d \rho_m + \left(k'_2 \frac{e}{T} + k_3 \frac{e}{T^2} \right) Z_v^{-1} \\ &= N_h + N_w \end{aligned} \quad (3.36)$$

The first term, N_h is the hydrostatic refractivity. The second term, N_w is the hydrostatic refractivity, but usually this is called **wet refractivity**, although this term is often also used for the earlier defined N_v .

3.4 ATMOSPHERIC PROFILES

In this section **theoretical profiles** are given for

- The temperature, dry-air, pressure, and the partial pressure of water vapor in saturated air.
- Based on the first two, a refractivity profile is given of dry air

As we have seen in the previous section,

- The propagation delay depends on the refractivity and the ray path,
- The refractivity and its turn depends on temperature and pressure.

To determine the **propagation delay**, we therefore need information on the temperature and pressure along the ray path. Although real profiles of temperature, pressure, refractivity, and partial pressure of water vapor can only be determined by actual measurements, obtained by, for example, radiosondes, idealized or standard profiles can be given based on the **temperature lapse rate** and theoretical assumptions.

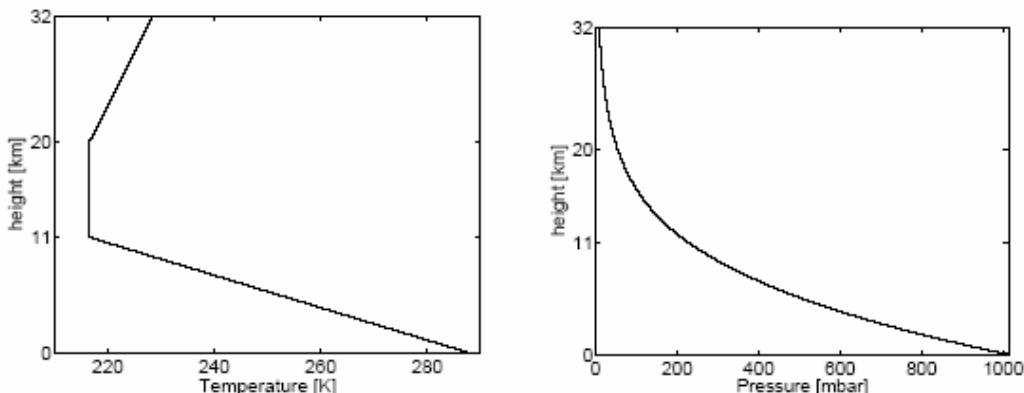


Figure 3.7 Temperature and dry pressure in the 1976 US Standard Atmosphere

Figure 4.7 shows a model temperature profile of the neutral atmosphere. The troposphere is characterized by a decreasing temperature. The measure of decrease $\beta = -\frac{dT}{dh}$ is called **lapse rate**. The lapse rate varies throughout the atmosphere, but is frequently constant in thick layers (Haltiner and Martin, 1957). For the derivation of a pressure profile we need to know the temperature profile. The variation is based on the dry-air different equation:

$$\frac{1}{P_d} dP = -\frac{g_m}{R_d T} dh, \quad (3.37)$$

which is obtained by the equation off state Eq.(1), the assumption of hydrostatic eqilibrium Eq.(4.2). We consider the **gravitation** to be constant with height and equal to a mean value:

$$g_m = \frac{\int_{h_0}^{\infty} \rho_m(h) g(h) dh}{\int_{h_0}^{\infty} \rho_m(h) dh} \quad (3.38)$$

For the **Isothermal layers** like troposphere, the pressure profile is found by integration of Eq.(37):

$$P_d = P_{d0} \exp\left(-\frac{h-h_0}{H}\right); \quad H \equiv \frac{R_d T}{g_m}, \quad (3.39)$$

P_{d0} : pressure of dry air at the base of the layer [mbar];

h : height above msl [km];

h_0 : height above msl at the base of the layer [km];

H : scale height [km]

In the case of a **polytropic layer** like the protosphere and stratosphere, with assumption of a constant lapse rate,

$$P_d = P_{d0} \left(\frac{T}{T_0} \right)^{\mu+1}, \quad \mu = \frac{g_m}{R_d \beta} - 1, \quad (3.40)$$

T_0 : temperature at the base of the layer [K]

Troposphere delay models often use standard values for the temperature and pressure. An example of a **standard atmosphere** is the 1976 US Standard Atmosphere in Table 3.2 (Stull,1995)

Table 3.2

troposphere: $T = 288.15 - 6.5h$	$0 < h < 11$ km;
tropopause: $T = 216.65$	$11 < h < 20$ km;
stratosphere: $T = 216.65 + h - 20$	$20 < h < 32$ km;
troposphere: $P_d = 1013.25(288.15/T)^{-5.255877}$	$0 < h < 11$ km;
tropopause: $P_d = 226.32 \exp(-0.1568(h-11))$	$11 < h < 20$ km;
stratosphere: $P_d = 54.749(216.65/T)^{34.16319}$	$20 < h < 32$ km.

3.4.1 Refractivity profile of dry air

From Eq.(3.33), (3.39), and (3.40), we can also derive the ***critical refractivity*** profiles of dry air. For polytropic layers we have

$$\frac{N_d}{N_{d0}} = \frac{k_1 P_d / T}{k_1 P_{d0} / T_0} = \frac{P_d}{P_{d0}} \frac{T_0}{T} = \left(\frac{T}{T_0} \right)^\mu, \quad (3.41)$$

N_{d0} : dry refractivity at the base of layer [-]

In Fig.3.8, the refractivity profiles is given for the 1976 US Standard Atmosphere

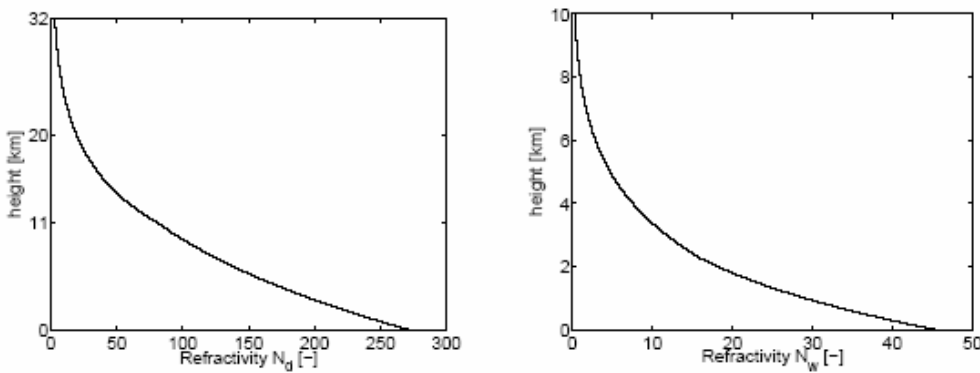


Figure 3.8 Refractivity profiles. Left: dry-air refractivity profile of the US Standard Atmosphere
Right: Wet-air refractivity profile for a surface pressure of 15°C, a constant relative humidity of 50% , a lapse rate of 6.5 K/ km, and constants of (Thayer, 1974).

Profiles of the hydrostatic refractivity are nearly the same as as these of dry air. Instead of for real temperature we have to assume a profile for the ***lapse rate of the virtual temperature*** in the formulas above. The virtual temperature is only the same as the real temperature for a mixing ratio of 0.

3.4.2 Saturation pressure profile

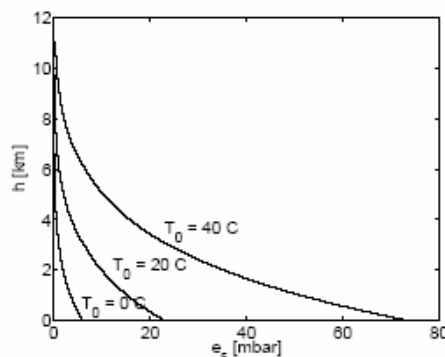


Figure 3.9 Profiles of saturated water-vapor pressure at different surface temperature for a lapse rate 6.5 K/ km and $h_0 = 0$

From model (3.22) and the assumption of a constant lapse rate, the partial pressure of saturated air is given as a function of height by:

$$e_{sat} = \exp \left[A - \frac{B}{T_0 - \beta(h - h_0)} \right], \quad (3.42)$$

e_{sat} : partial pressure saturated air

T_0 : surface temperature [K]

h_0 : height of the surface above msl [km]

Since hardly any water vapor is present in or above the tropopause, it is sufficient to consider only a **tropospheric profile**. Three different profiles are given in Fig.3.9. Fig. 3.9 shows an example of a wet refractivity profile based on Eq.(3.42).

The **thickness of the troposphere** is often exposed by the **effective height**, refractivity weighted mean height:

$$H_m = \frac{\int_{h_0}^{\infty} (h - h_0) N(h) dh}{\int_{h_0}^{\infty} N(h) dh}$$

For exponential profiles, the effective height is equal to scale height. The effective height of the dry and wet troposphere is about 8 km and 20 km respectively. The latter value holds if the relative humidity is independent of height as in Fig.3.8.

- The smaller effective height of the weight troposphere causes the wet refractivity to drop much faster with increasing altitude than the dry refractivity.
- The contribution of the wet part to the total refractivity is therefore at high altitudes smaller than the surface.

CHAPTER 4:

PHYSICS OF IONOSPHERE

4.1 HISTORY

In 1899, in a landmark experiment on December 12, 1901, Marconi, who is often called the "Father of Wireless," demonstrated transatlantic communication by receiving a signal in St. John's Newfoundland that had been sent from Cornwall, England. Because of his pioneering work in the use of electromagnetic radiation for radio communications, Marconi was awarded the Nobel Prize in physics in 1909.

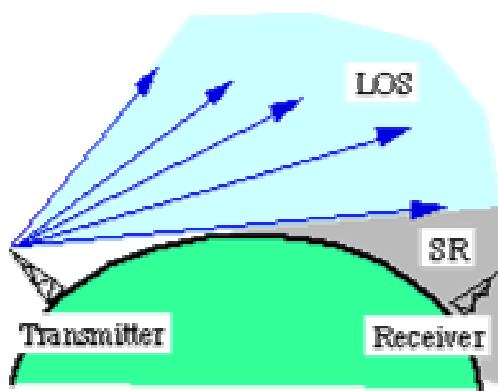


Figure 4.1 Areas in the light blue region are within the radio "Line of Sight" (LOS). The receiving antenna is in the shadow region (SR) and cannot receive a signal directly from the transmitter.

Marconi's famous experiment showed the way toward world wide communication, but it also raised a serious scientific dilemma. Up to this point, it had been assumed that electromagnetic radiation travelled in straight lines in a manner similar to light waves. If this were true, the maximum possible communication distance would be determined by the geometry of the path as shown in Fig.4.1 to the left.

The radio signal would be heard up to the point where some intervening object blocked it. If there were no objects in the path, the maximum distance would be determined by the transmitter and receiver antenna heights and by the bulge (or curvature) of the earth. Drawing from light as an analogy, this distance is often called the "**Line-of-Sight**" (LOS) distance. In Marconi's transatlantic demonstration, something different was happening to cause the radio waves to apparently bend around the Earth's curvature so that the communication signals from England could be heard over such an unprecedented distance.

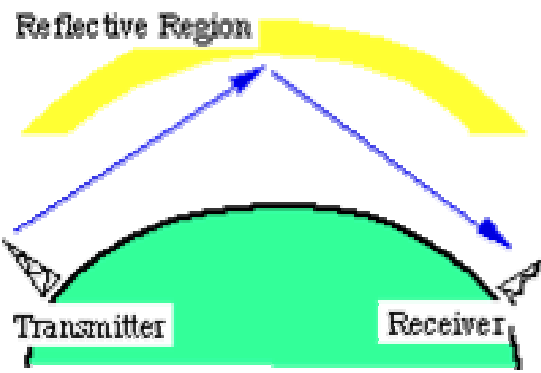


Figure 4.2 A conductive region at high altitude would "reflect" radio signals that reached it and return them to Earth.

In 1902, Oliver Heaviside and Arthur Kennelly each independently proposed that a conducting layer existed in the upper atmosphere that would allow a transmitted EM signal to be reflected back toward the Earth. Up to this time, there was no direct evidence of such a region and little was known about the physical or electrical properties of the Earth's upper atmosphere. If such a conductive layer existed, it would permit a dramatic extension of the "line-of-Sight" limitation to radio communication as shown in Fig.4.2. to the left.

During the mid-1920's, the invention of the **ionosonde** allowed direct observation of the ionosphere and permitted the first scientific study of its characteristics and variability and its affect on radio waves.

4.2 REQUIREMENTS FOR AN IONOSPHERE

For a PLANETARY IONOSPHERE: The only requirements are a neutral atmosphere and a source of ionization for the gases in that atmosphere. Sources of ionization include photons and energetic particle "precipitation". The process involving the former is referred to as photoionization, the latter is often labeled impact ionization.



Figure 4.3 The conceptual drawing is a simplified explanation of ionization process.

Solar photons in the extreme ultraviolet (EUV) and ultraviolet(UV) wavelength range of approximately 10nm to 100 nm typically produce at least the dayside ionosphere of the planets.

The photons come from primarily from the Sun. Ionizing particles can come from galaxy(cosmic rays), the Sun, the magnetosphere, and the ionosphere itself if a process for local ion or electron acceleration is operative. Precipitating energetic electrons produce additional ionizing photons within the atmosphere by a process known as bremsstrahlung or breaking radiation.

The only requirement on the ionizing photons and particles is that their energies, i.e., $h\nu$ in the case of photons, and kinetic energy in case of particles exceed the ionization potential or binding of a neutral-atmosphere atomic or molecular electron. In nature, atmospheric ionization usually is attributable to a mixture of these various source, but often one dominates

4.3 THE NEUTRAL ATMOSPHERE

The density n_i of a constituent of the upper neutral atmosphere obeys a hydrostatic equation:

$$n_i m_i g = -\frac{dP}{dh} = -\frac{d}{dh}(n_i kT_i) \quad (4.1)$$

which expresses as a balance between the vertical gravitational force and the thermal-pressure-gradient force on the atmospheric gas.

Here,

m_i :molecular or atomic mass,

g : the acceleration due to gravity,

h :altitude variable,

and

P :the thermal pressure, $n_i kT_i$

k :Boltzmann's constant,

T_i : temperature of the neutral gas under consideration

If T_i is assumed independent of h ,this equation has the exponential solution

$$n_i = n_0 \exp \frac{-(h-h_0)}{H_i} \quad (4.2)$$

where $H_i = kT_i/m_i g$ defines the scale height of the gas, and n_0 the density at the reference altitude h_0 .

Note that the scale-height dependence on particle mass is such that the lightest molecules and atoms have the largest scale-height.

Most planetary atmospheres are dominated at high altitude by hydrogen and helium. Of course, T_i may depend on h , so that this simple exponential distribution will not always provide an accurate description.

4.4. ION PRODUCTION.

Some simplifying assumptions can be made that together will allow an analytical approach to ionosphere modeling known as ***Chapman theory***.

In Chapman theory, the goal is to describe ion production as a function of height for the simple case in which the details of photon absorption are hidden in a radiation-absorption cross section σ and in which ion production is assumed to depend only on the amount of radiative energy absorbed.

We define the following variables:

n_i : density of neutrals (per cubic meter)

h : height

I : intensity of radiation (energy flux, electron volts per square meter per second)

σ : photon-absorption cross section (square meter).

Q : rate of ion production (photoionization rate, electrons per cubic meter per second)

s : line-of-sight path length

χ : zenith angle

C : number of electrons produced in the absorber per unit energy absorbed (electrons per electron volt).

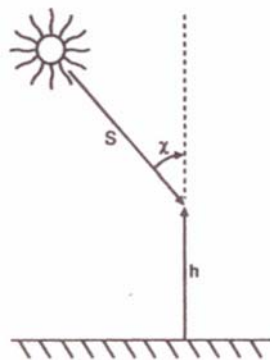


Figure 4.4: Illustration showing the line-of-sight path length s , the solar zenith angle χ , and the altitude h are illustrated

The atmosphere is presumed to be exponential, planar, and horizontally stratified. Assumptions that are idealization of the real world, where atmospheres are only approximately exponential and curved, and the scale height H_i depends on χ . As radiation is absorbed, its intensity decreases.

$$-\frac{dI}{ds} = \sigma n_i I \quad (4.3)$$

Because the rate of ion production should be proportional to the rate at which radiation is absorbed, we can write

$$Q = -C \frac{dI}{ds} = \sigma C n_i I \quad (4.4)$$

where C is the constant of proportionality (approximately 1 ion pair per 35 eV in air).

For the peak or maximum of production(subscript m),

$$\frac{dQ}{ds} = 0$$

where s is related to h by $ds = -dh \sec \chi$ (Fig.4.4).

$$\sigma H_i n_m \sec \chi = 1 \quad (4.5.a)$$

$$\sigma N_{im} = 1 \quad (4.5.b)$$

where N_{im} is the integrated density $\int_{\infty}^{S_m} n_i ds$ along the line-of-sight up to the position of the peak S_m .

Useful term is **optical depth** τ , which describes the attenuation of the ionizing radiation. The optical depth arises naturally in the expansion for intensity at positions along the line-of-sight relative to the intensity at infinity.

Integrating, (4.3)

$$\ln \left(\frac{I(s)}{I(\infty)} \right) = -\sigma \int_{\infty}^s n_i ds = -\sigma N_{is}$$

or

$$I(s) = I(\infty) \exp(-\sigma N_{is}) = I(\infty) \exp(-\tau)$$

At the peak, $\sigma N_{is} = \sigma N_{im} = 1$; so the peak is the altitude where the optical depth is unity. We shall call $I(\infty)$ instead of $I(0)$, because the former is standard nomenclature.

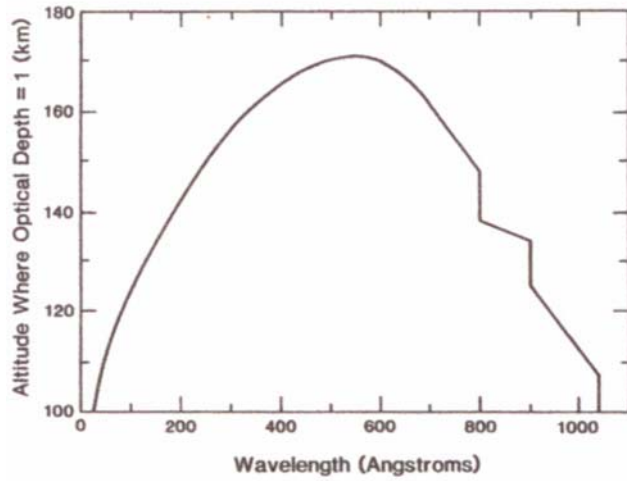


Figure 4.5: Photonwavelength versus the altitude in the Earth's atmosphere

The altitudes at which photons of various wavelengths reach unit optical depth in the Earth's atmosphere are illustrated in Fig.4.5.

Now we return to the analysis of the radiation rate Q . The peak production rate is

$$Q_m = C\sigma n_m I_m = C\sigma(\sigma H_i \sec \chi)^{-1}(I(\infty) \exp(-1)) = \frac{CI(\infty) \cos \chi}{H_i} \exp(1) \quad (4.6)$$

Given the neutral-gas altitude profile $n_i = n_0 \exp(-(h - h_0)/H_i)$, we can determine the height of the production peak h_m by writing

$$\sigma H_i n_m \sec \chi = 1 = \sigma H_i n_0 \exp\left(\frac{-(h_m - h_0)}{H_i}\right) \sec \chi \quad (4.7)$$

)

and solving for h_m .

Similarly, we can determine the dependence of the radiation intensity on h by using the earlier expression for $I(s)$ and noting that N_{is} is the integrated density along the line of sight:

$$I(h) = I(\infty) \exp\left[-\sigma n_0 H_i \sec \chi \exp\left(\frac{-(h - h_0)}{H_i}\right)\right] \quad (4.8)$$

The dependence of the production rate Q on h, s is then given by

$$Q = Q_m \exp \left[1 + \frac{(h_m - h_0)}{H_i} - \exp \left(\frac{(h_m - h_0)}{H_i} \right) \right] \quad (4.9a)$$

with $CI(\infty) = Q_m \exp(1) H / \cos \chi_i$.

This can be simplified by defining $y = (h - h_0)/H_i$, hence

$$Q = Q_m [1 - y - \exp(-y)] \quad (4.9b)$$

which is the **Chapman production function**. Note that far above the peak ($y \geq 2$), a good approximation is

$$Q \propto \exp(-y) \quad (4.9c)$$

which says that because the radiation intensity is practically constant at high altitudes (not much absorption occurs), Q is proportional to neutral density. The rate Q is the rate of production of ions and photoelectrons, because these usually are produced in pairs most of ions are singly ionized in this process. It is notable that in the expansion for Q , the proton-absorption cross section does not explicitly appear. The properties of the absorber are contained in the constant C

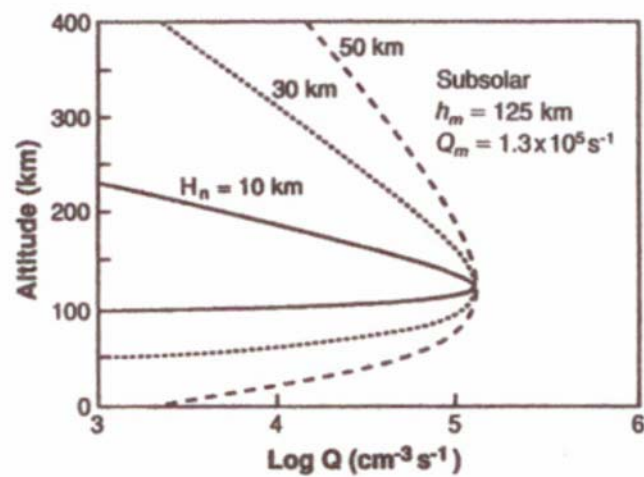


Figure 4.6: Chapman production function

The subsolar ($\chi=0$) Chapman production function or ion production profile in atmospheres with several different scale heights is plotted in Fig.4.6.. Our derivation of the Chapman production function has assumed a flat earth in which the solar zenith angle has a fixed value.

4.5 PARTICLE IMPACT IONIZATION

In many situations of interest, solar photons can be assumed to compose the dominant source of atmosphere ionization. However, an occasion, energetic (energies ≥ 1 keV) precipitating charged particles are important. This can occur, for example, during the night magnetic latitudes in the case of planets with dipolar magnetic field and satellites with atmospheres submerged in planetary atmospheres,

One simplified approach for particle impact ionization involves the use of an empirically determined function $R(\xi_0)$ called the **range-energy relation**.

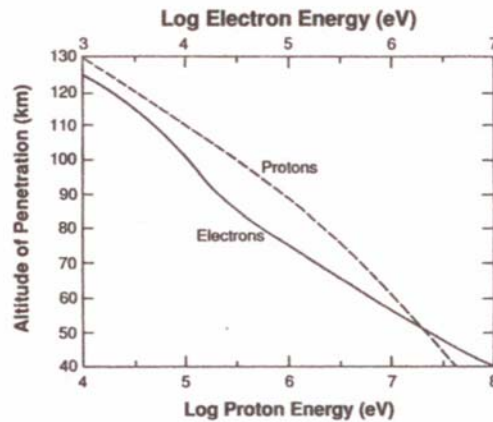


Figure 4.7: Penetration altitudes for electron and protons

The range-energy relation $R(\xi_0)$ is also defined by the integral

$$R(\xi_0) = - \int_0^{\xi_0} \frac{d\xi}{d\xi/dx} \quad (4.14)$$

where $d\xi/dx$ is the energy lost per gram per square centimeter traversed.

Suppose we postulate that the depth of matter x traversed at any point in the particle's transit can be approximated by

$$x = - \int_{\xi_{loc}}^{\xi_0} \frac{d\xi}{d\xi/dx} = R(\xi_0) - R(\xi_{loc}) \quad (4.15)$$

where ξ_{loc} is energy at x . Because $R(\xi_0)$ has the general functional form

$$\xi_{loc} = \left[\frac{1}{A} (A \xi_0^\gamma - x) \right]^{1/\gamma} \quad (4.16)$$

It follows that the energy deposited at a given x is

$$\frac{d\xi}{dx} = -\frac{\xi_{loc}^{1-\gamma}}{A\gamma} \quad (4.17)$$

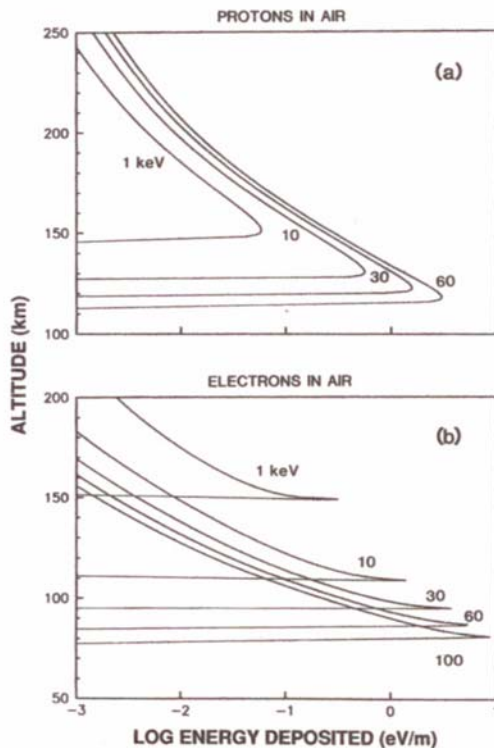


Figure 4.8: Energy deposition profiles

The altitude profile of $\frac{d\xi_{loc}}{dx}$ times the local-atmosphere mass density $\rho(h)$ gives the energy deposition in

electron volts per meter for the particle at x. The curve of $\rho(x) \frac{d\xi_{loc}}{dx}$ versus is then the needed profile.

Some example obtained with the foregoing expression for $R(\xi_0)$ in air assuming the density profile for the earth's atmosphere are shown in Fig.4.8. Because the incident particles have a distribution of energies described by a flux pectrum $J(E_0)$ (particles.cm⁻².s), a total energy-deposition profile can be built up by weighing the profiles for the single particles by $J(E_0)$, giving the energy deposition in electronvolt-seconds per cubic centimeter.

Finally for a particular gas mixture, one uses an empirically determined value for the energy required to produce an ion pair. Divison of the energy deposition profile by this constant gives the ion production profile (in ions produced per cubic centimeter per second versus altitude) for the incident-particle flux described $J(E_0)$. Because the incident particles have a distribution of energies described by a flux

spectrum $J(E_0)$ (particles.cm⁻².s), a total energy-deposition in electrovolt-seconds per cubic centimeter. For air, approximately 35 eV will produce an ion pair.

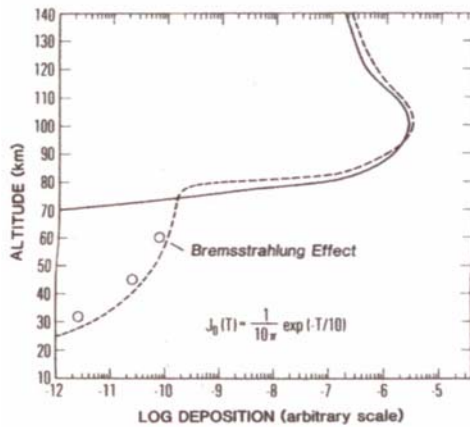


Figure 4.9

Fortunately, this nonsolar source of photoionization usually is unimportant, except at the lowest ionospheric altitudes, and as illustrated Fig.4.9, the ion density it produces is well below the peak density produced by the precipitating particles. It is usually justifiable to neglect it except in special cases (such in atmospheric-chemistry problems, which are sensitive to the local rates of ion production in the earth's middle atmosphere).

4.6 ION LOSS

Once the ion production rate is known, the next critical quantity that must be specified for the ionospheric model is the ion or electron loss rate L . Ionospheric electrons disappear by virtue of three types of recombination:

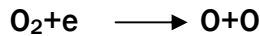


The first of two of these are important throughout the bulk of the ionosphere. Radiative recombination is responsible for many types of observed airglows. In contrast, most of the emission that one sees in an aurora occurs when atomic and molecular electrons are excited to high energy levels by Coulomb collisions with the passing precipitating particles and then undergo radiation re-excitation,

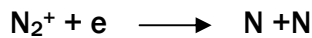
Recombination occurs at rates that depend on the local concentrations of the ions and electrons

$$L = \alpha n_e n_i$$

where n_e and n_i are the electron and ion densities, and α is recombination coefficient is determined by empirical and theoretical models. For the more important atmospheric dissociative recombination reactions, such as



and



It is notable that α is often assumed constant, although T_e generally depends on altitude.

4.7 DETERMINING IONOSPHERIC DENSITY FROM PRODUCTION AND LOSS RATE

Once the ion production rates and loss rates are established , we can consider the problem of finding the altitude distribution of the ionospheric electron density n_e . If the electrons and ions do not move very far from where they are produced (e.g., by virtue of a strong horizontal ambient magnetic field), we can say that n_e (and thus n_i) obeys the equilibrium-continuity or particle-conservation equation

$$\frac{dn_e}{dt} = Q - L = 0 \quad (4.18)$$

and if the loss rate is due to electron-ion collisions

$$Q = L = \alpha n_e^2$$

and hence

$$n_e = (Q/\alpha)^{1/2} \quad (4.19)$$

describes the spatial distribution of the electrons or ions. This particular distribution is called ***photochemical equilibrium distribution*** because it involves only local photochemistry. Chapman-layer models of the ionosphere, for example, include the Chapman production function and the assumption of photochemical equilibrium. However, in many cases the electrons and ions move significantly from their points of creation before they recombine, and so we must consider a transport term in a more general continuity equation.

CHAPTER 5:

ATMOSPHERIC WAVE PROPAGATION

5.1 RADIO WAVE PROPAGATION CHARACTERISTICS

Within the atmosphere, radio waves can be refracted, reflected, and diffracted. In the following sections, we will first recall history and then discuss the propagation characteristics in atmosphere.

5.1.1 REFRACTION

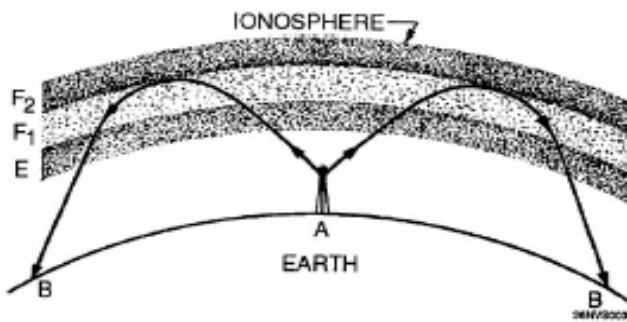


Figure 5.1 Radio-wave refraction

A radio wave transmitted into ionized layers is always refracted, or bent. This bending of radio waves is called **refraction**. Notice the radio wave shown in Fig.5 1, traveling through the earth's atmosphere at a constant speed.

As the wave enters the denser layer of charged ions, its upper portion moves faster than its lower portion. The abrupt speed increase of the upper part of the wave causes it to bend back toward the earth. This bending is always toward the propagation medium where the radio wave's velocity is the least. The amount of refraction a radio wave undergoes depends on three main factors:

- 1) The ionization density of the layer
- 2) The frequency of the radio wave
- 3) The angle at which the radio wave enters the layer

5.1.1.1 Layer density

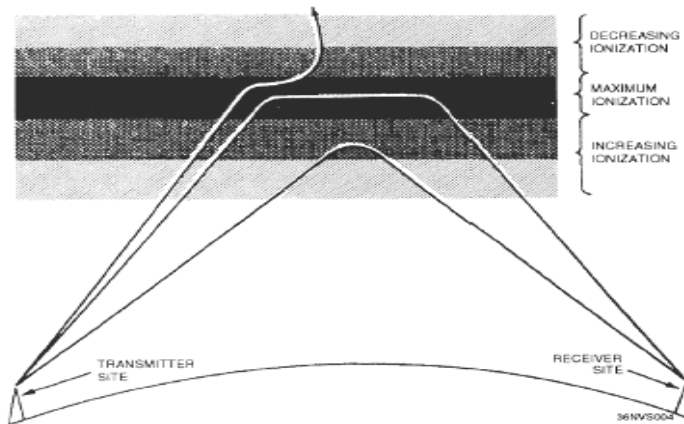


Figure 5.2 Effects of ionospheric density on radio waves

Fig. 5.2 shows the relationship between radio waves and ionization density. Each ionized layer has a middle region of relatively dense ionization with less intensity above and below. As a radio wave enters a region of increasing ionization, a velocity increase causes it to bend back toward the earth. In the highly dense middle region, refraction occurs more slowly, because the ionization density is uniform. As the wave enters the upper less dense region, the velocity of the upper part of the wave decreases and the wave is bent away from the earth.

5.1.1.2 Frequency

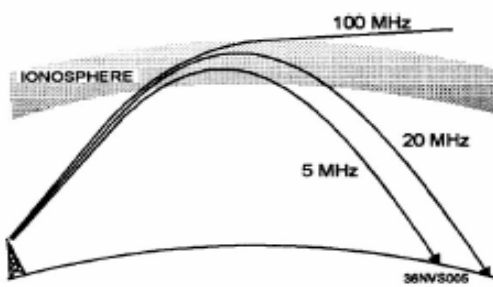


Figure 5.3 Frequency versus refraction and distance

The lower the frequency of a radio wave, the more rapidly the wave is refracted by a given degree of ionization. Fig. 5.3. shows three separate waves of differing frequencies entering the ionosphere at the same angle.

- You can see that the 5-MHz wave is refracted quite sharply, while the 20-MHz wave is refracted less sharply and returns to earth at a greater distance than the 5-MHz wave.

- Notice that the 100-MHz wave is lost into space. Since the 100-MHz wave's frequency is greater than the critical frequency for that ionized layer.

For any given ionized layer, there is a frequency, called the **escape point**, at which energy transmitted directly upward will escape into space. The maximum frequency just below the escape point is called the **critical frequency**. The critical frequency of a layer depends upon the layer's density. If a wave passes through a particular layer, it may still be refracted by a higher layer if its frequency is lower than the higher layer's critical frequency.

5.1.1.3 Angle of Incidence and Critical angle

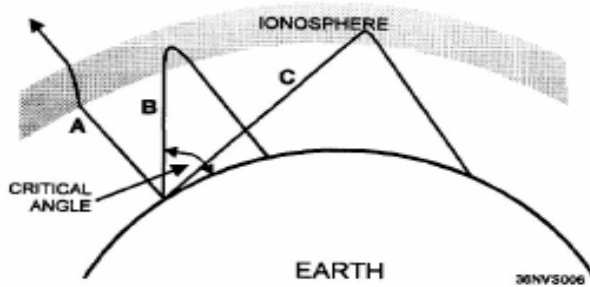


Figure 5.4 Incidence angles of radio waves

When a radio wave encounters a layer of the ionosphere, that wave is returned to earth at the same angle (roughly) as its **angle of incidence**. Fig. 5.4 shows three radio waves of the same frequency entering a layer at different incidence angles.

- The angle at which wave A strikes the layer is too nearly vertical for the wave to be refracted to earth. Since any wave, at a given frequency, that leaves the antenna at an incidence angle greater than the **critical angle** will be lost into space.
- However, wave B is refracted back to earth. The angle between wave B and the earth is called the **critical angle**.
- Wave C leaves the antenna at the smallest angle that will allow it to be refracted and still return to earth. The critical angle for radio waves depends on the layer density and the wavelength of the signal.

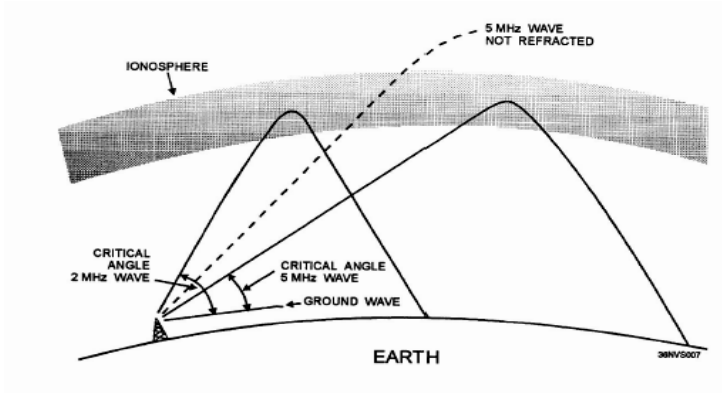


Figure 5.5 The effect of frequency on the critical angle

As the frequency of a radio wave is increased, the critical angle must be reduced for refraction to occur. Notice in Fig.5.5 that the 2-MHz wave strikes the ionosphere at the critical angle for that frequency and is refracted. Although the 5-MHz line (broken line) strikes the ionosphere at a less critical angle it still penetrates the layer and is lost. As the angle is lowered, a critical angle is finally reached for the 5-MHz wave and it is refracted back to earth.

5.1.2 REFLECTION

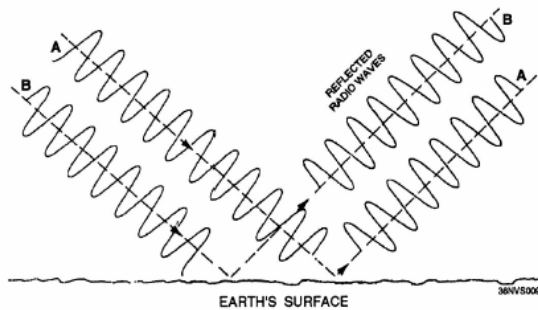


Figure 5.6 Phase shift of reflected waves

Reflection occurs when radio waves are “bounced” from a flat surface. There are basically two types of reflection that occur in the atmosphere: earth reflection and ionospheric reflection.

Fig.5.6 shows two waves reflected from the earth’s surface. Waves A and B bounce off the earth’s surface like light off of a mirror. Notice that the positive and negative alternations of radio waves A and B are in phase before they strike the earth’s surface. However, after reflection the radio waves are approximately 180 degrees out of phase. **A phase shift** has occurred.

- The amount of phase shift that occurs is not constant. It varies, depending on the wave polarization and the angle at which the wave strikes the surface..

- Normally, radio waves reflected in phase produce stronger signals, while those reflected out of phase produce a weak or fading signal.

For ionospheric reflection to occur, the highly ionized layer can be approximately no thicker than one wavelength of the wave.

- Although the radio waves are actually refracted, some may be bent back so rapidly that they appear to be reflected.
- Since the ionized layers are often several miles thick, ionospheric reflection mostly occurs at long wavelengths (low frequencies).

5.1.3 DIFFRACTION

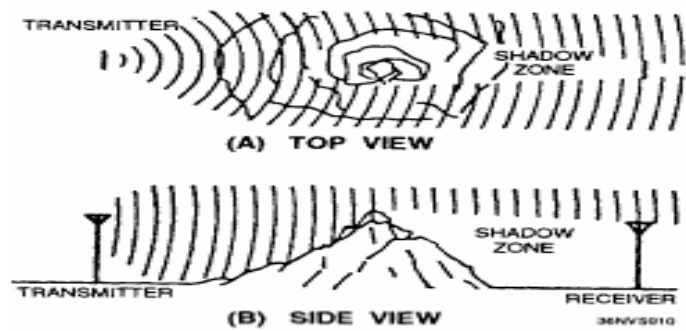


Figure 5.7 Diffraction around an object

Diffraction is the ability of radio waves to turn sharp corners and bend around obstacles. As shown in Fig.5.7 , diffraction results in a change of direction of part of the radio-wave energy around the edges of an obstacle. Radio waves with long wavelengths compared to the diameter of an obstruction are easily propagated around the obstruction.

However, as the wavelength decreases, the obstruction causes more and more attenuation, until at very-high frequencies a definite **shadow zone** develops. The shadow zone is basically a blank area on the opposite side of an obstruction in **line-of-sight** from the transmitter to the receiver. Diffraction can extend the radio range beyond the horizon. By using high power and low-frequencies, radio waves can be made to encircle the earth by diffraction.

5.1.4 ABSORBTION AND SCATTERING

As a radio wave passes into the ionosphere, it loses some of its energy to the free electrons and ions present there. Since the amount of **absorption** of the radio-wave energy varies with the density of the ionospheric layers, there is no fixed relationship between distance and signal strength for ionospheric propagation.

Energy absorbed from the incident wave by the charged particle is re-emitted as radio wave radiation. Such a process is clearly equivalent to the **scattering** of the radio wave by the particle.

5.2. ATMOSPHERIC EFFECTS ON PROPAGATION

While radio waves traveling in free space have little outside influence to affect them, radio waves traveling in the earth's atmosphere have many influences that affect them. We have all experienced problems with radio waves, caused by certain atmospheric conditions complicating what at first seemed to be a relatively simple electronic problem. These problem-causing conditions result from a lack of uniformity in the earth's atmosphere. Many factors can affect atmospheric conditions, either positively or negatively. Three of these are variations in geographic height, differences in geographic location, and changes in time (day, night, season, year).

Changes in the ionosphere can produce dramatic changes in the ability to communicate. In some cases, communications distances are greatly extended. In other cases, communications distances are greatly reduced or eliminated. The paragraphs below explain the major problem of reduced communications because of the phenomena of **fading** and **selective fading**.

Although daily changes in the ionosphere have the greatest effect on communications, other phenomena also affect communications, both positively and negatively. Those phenomena are discussed briefly in the following sections.

5.2.1 REGULAR VARIATONS

5.2.1 1 FADING

The most troublesome and frustrating problem in receiving radio signals is variations in signal strength, most commonly known as **fading**. Several conditions can produce fading.

- When a radio wave is refracted by the ionosphere or reflected from the earth's surface, random changes in the polarization of the wave may occur.
- Fading also results from absorption of the RF energy in the ionosphere. Most ionospheric absorption occurs in the lower regions of the ionosphere where ionization density is the greatest.

5.2.1.2. MULTIPATH

Multipath is simply a term used to describe the multiple paths a radio wave may follow between transmitter and receiver. Such propagation paths include the ground wave, ionospheric refraction, reradiation by the ionospheric layers, reflection from the earth's surface or from more than one ionospheric layer, and so on.

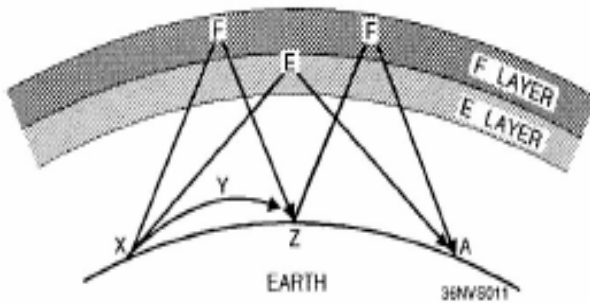


Figure 5.8 Multiple transmission

Fig.5.8 shows a few of the paths that a signal can travel between two sites in a typical circuit.

- One path, XYZ, is the basic ground wave.
- Another path, XFZ, refracts the wave at the F layer and passes it on to the receiver at point Z.
- At point Z, the received signal is a combination of the ground wave and the sky wave. These two signals, having traveled different paths, arrive at point Z at different times. Thus, the arriving waves may or may not be in phase with each other.
- A similar situation may result at point A.
- Another path, XEA, results from a greater angle of incidence and two refractions from the F layer.
- A wave traveling that path and one traveling the XEA path may or may not arrive at point A in phase. Radio waves that are received in phase reinforce each other and produce a stronger signal at the receiving site, while those that are received out of phase produce a weak or fading signal.

5.2 1 .3 SEASONAL VARIATIONS IN THE IONOSPHERE

Seasonal variations are the result of the earth's revolving around the sun, because the relative position of the sun moves from one hemisphere to the other with the changes in seasons.

- Seasonal variations of the D, E, and F1 layers are directly related to the highest angle of the sun, meaning the ionization density of this layer is greatest during the summer.
- The F2 layer is just the opposite. Its ionization is greatest during the winter, Therefore, operating frequencies for F2 layer propagation are higher in the winter than the summer.

5.2. 1 4 SUNSPOTS

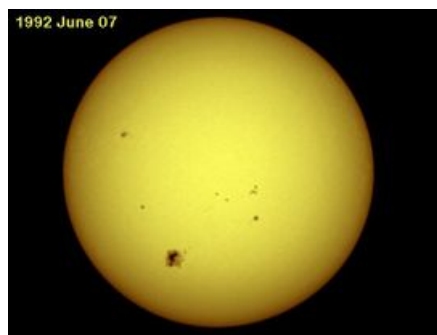


Figure 5.9 Sunspots on the Sun's surface

The appearance and disappearance of dark, irregularly shaped areas known as **sunspots** are characterized by strong magnetic fields. These sunspots cause variations in the ionization level of the ionosphere. Sunspots tend to appear in two cycles, every 27 days and every 11 years.

5.2.1 4.1 Twenty-Seven Day Cycle

As the sun rotates on its own axis, these sunspots are visible at 27-day intervals, which is the approximate period for the sun to make one complete revolution. During this time period, the fluctuations in ionization are greatest in the F2 layer. For this reason, calculating critical frequencies for long-distance communications for the F2 layer is not possible and allowances for fluctuations must be made.

5.2.1 4.2 Eleven-year cycle

Sunspots can occur unexpectedly, and the life span of individual sunspots is variable. The **eleven-year sunspot cycle** is a regular cycle of sunspot activity that has a minimum and maximum level of activity that occurs every 11 years. During periods of maximum activity, the ionization density of all the layers increases. Because of this, the absorption in the D layer increases and the critical frequencies for the E, F1, and F2 layers are higher. During these times, higher operating frequencies must be used for long-range communications.

5.2.2 .IRREGULAR VARIATIONS

Irregular variations are just that unpredictable changes in the ionosphere that can drastically affect our ability to communicate. The more common variations are sporadic E, ionospheric disturbances, and ionospheric storms

5.2.2.1 Sporadic E

The sporadic E layer can be so thin that radio waves penetrate it easily and are returned to earth by the upper layers, or it can be heavily ionized and extend up to several hundred miles into the ionosphere. This condition may be either harmful or helpful to radio-wave propagation.

5.2.2.2 Sudden ionospheric disturbances

Commonly known as SID, these disturbances may occur without warning and may last for a few minutes to several hours. When SID occurs, long-range hf communications are almost totally blanked out. The radio operator listening during this time will believe his or her receiver has gone dead.

5.2.2.3 Ionospheric storms

Ionospheric storms are caused by disturbances in the earth's magnetic field. They are associated with both solar eruptions and the 27-day cycle, meaning they are related to the rotation of the sun.

The effects of ionospheric storms are a turbulent ionosphere and very erratic sky-wave propagation, reducing its ion density and causing the critical frequencies to be lower than normal.

5.3. WEATHER

Wind, air temperature, and water content of the atmosphere can combine either to extend radio communications or to greatly attenuate wave propagation making normal communications extremely difficult.

5.3.1 Rain

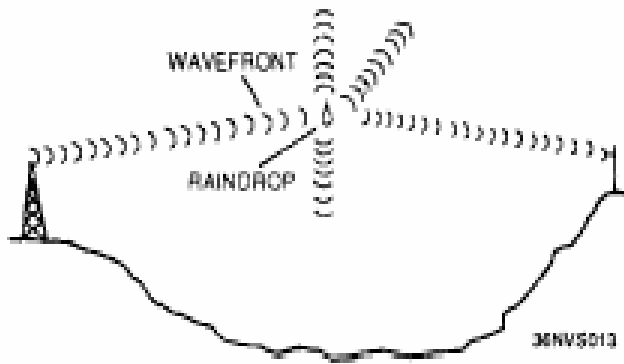


Figure 5.10 RF energy losses from scattering

Attenuation because of raindrops is greater than attenuation for any other form of precipitation. (Fig.5.10). Raindrops cause greater attenuation by scattering than by absorption at frequencies above 100 MHz. At frequencies above 6 GHz, attenuation by raindrop scatter is even greater.

5.3.2 Fog

Attenuation because of fog has little effect on frequencies lower than 2 GHz, but can cause serious attenuation by absorption at frequencies above 2 GHz.

5.3.3 Snow

Because of the irregular shape low density of the snowflake and, the scattering and absorption losses are difficult to compute, but will be less than those caused by raindrops.

5.3.4 Hail

Attenuation by hail is determined by the size of the stones and their density. Attenuation of radio waves by scattering because of hailstones is considerably less than by rain.

REFERENCES

- 1.** Houghton, J. (200) The Physics of Atmosphere (1st Edition), Cambridge: Cambridge University Press.
- 2.** Gombosi, T.I. (1998) Physics of the Space Environment (3rd Edition) Cambridge: Cambridge University Press.
- 3.** The American Practical Navigator, An Epitome of Navigation(1995), originally by Nathaniel Bowditch, LL.D., 1995 Edition, published and prepared by National Imagery and Mapping Agency,Bethesda, Maryland.
- 4.** Kleijer, F. (2004) Troposphere Modeling and Filtering Precise for GPS Leveling, Publications on Geodesy 56, Netherlands Geodetic Commission, printed by Optima Grafische Communicatie, The Netherlands.